DOR: 20.1001.1.2322388.2021.9.1.5.1

Research Paper

Nanoporous Carbon Spheres Derived from the Leather Leaf as Electrode Materials for Supercapacitors

Azam Asadi[1], Hamid Oveisi[*1, 2]
1. Department of Materials and Polymer Engineering, Hakim Sabzevari University, Sabzevar 9617976487, Iran
2. Nanotechnology Research Center, Hakim Sabzevari University, Sabzevar 9617976487, Iran

ARTICLE INFO

Article history:

Received 2 August 2020
Accepted 2 October 2020
Available online 1 January 2021

Keywords:
Nanoporous Carbon
Biomass
Leather Leaf
Spherical Morphology
Supercapacitor

ABSTRACT

In this study, nanostructured carbon spheres were fabricated from leather leaf via hydrothermal carbonization and chemically activated with KOH. Different hydrothermal carbonization temperatures were used. The microtopographic, compositional, and structural characteristics and the surface properties of the synthesized material were then investigated via scanning electron microscopy, transmission electron microscopy, X-ray diffraction, nitrogen adsorption-desorption, and Raman spectroscopy. Results indicated that the KOH-activated sample synthesized with hydrothermal procedure leads to spheroidal nano-porous amorphous carbon particles with an average size of 3-5 micrometers. The nano-porous carbon spheres exhibited remarkable material properties such as high specific surface area (1342 m^2 g^{-1}) and a well-developed porosity with a distribution of micropores 2 nm wide. These properties led to good electrochemical performance as supercapacitor electrodes. The electrochemical investigations through a three-electrode cell in an aqueous electrolyte have also confirmed the capability of the synthesized activated carbon nano-particles as promising candidates for supercapacitor applications. In particular, a specific capacitance of 374 F g^{-1} was achieved at a current density of 2 A g^{-1}.

*** Corresponding Author:**
E-mail: hamid.oveisi@hsu.ac.ir

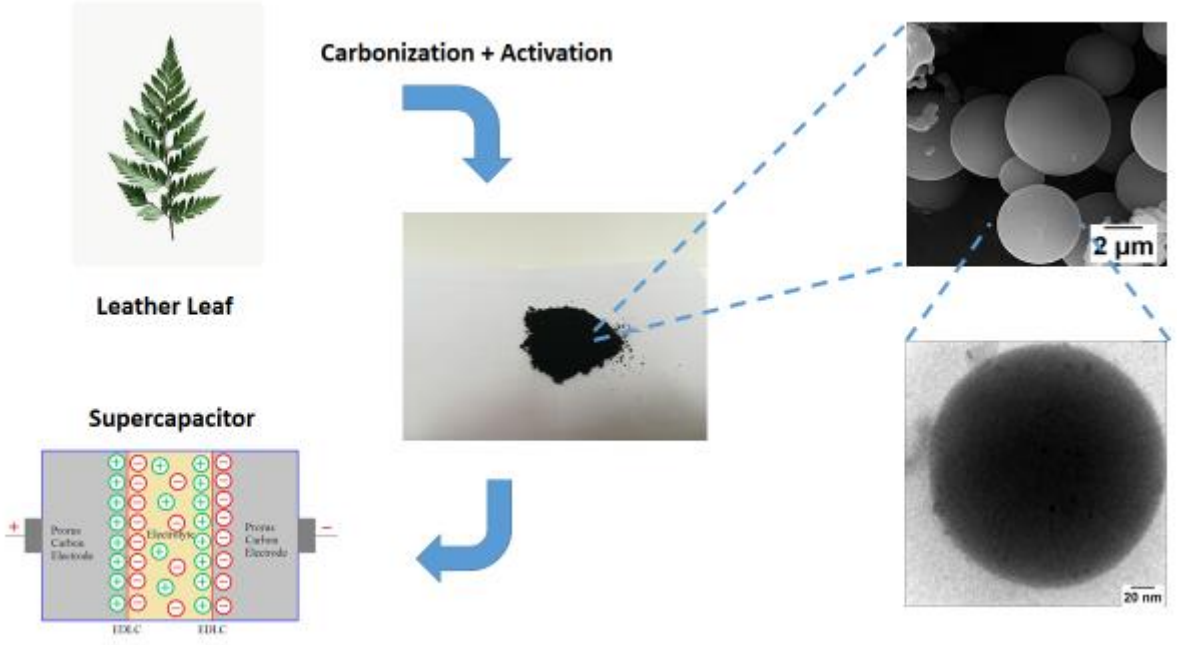

Graphical abstract of hydrothermal carbonization of nanoporous carbon spheres derived from the leather leaf

1- Introduction

The development of green, renewable, and highly efficient methods of energy conversion, as well as new energy storage technologies, is in high demand [1-3]. As an energy storage device, supercapacitors are an effective and practical technology for electrochemical energy conversion and storage. Supercapacitors, also known as EDLC (electric double-layer capacitors) or Ultracapacitors, can store tremendous amounts of energy. Operating based on their electrochemical properties, supercapacitors have found incredible recognition for novel applications. Their outstanding electrochemical performance, including optimal reversibility, power capability, and cycle life, makes them great options in different areas, such as intelligent automobiles, portable power tools, and uninterruptible power sources [4].

Fabricating supercapacitors requires cost-effective production materials. Carbonaceous materials, which are popular base materials for electrodes, are an incredible option since they provide an easy fabrication process, potentially significant specific capacitance, and considerable mechanical flexibility [5]. Among various carbonaceous materials, nanoporous carbon spheres have gained considerable attention due to their optimal electrical conductivity and the ability to minimize viscous effects and finely tune the porosity [6-8]. The discovery of fullerenes, carbon nanotubes, nano-porous carbon, and graphene, with optimal nanostructures and functionalization patterns, has made the areas related to advanced carbon materials mainly thriving. However, these carbon nanomaterials strongly depend on precursors based on fossil fuels, such as CH_4, phenol, and pitch, and extreme synthetic conditions requiring massive energy levels. These methods and techniques are not optimally cost-effective and can damage the environment because they use unsafe toxic compounds that are environmentally unfriendly. Hence, the development of nanoporous carbon derived from renewable biomass is of growing importance for creating sustainable energy-storage systems [9-14].

Hence, various synthetic strategies, including hydrothermal carbonization [15], nanocasting technique [16], and emulsion polymerization method [17], have been developed for the preparation of carbon spheres. In addition to the kinds of synthetic methods, carbon materials also can be fabricated by hydrothermal carbonization [18-21] for creating nanoporous carbon spheres.

In this work, we demonstrate a simple hydrothermal assisting pyrolysis method by using a green, renewable, cost-effective, and widespread plant as the precursors and explored as an electrode for supercapacitors. Due to its special characteristics, such as emulsifying, gelling, and stabilizing abilities, the leather leaf has been extensively used in medical and ornamental usage. However, to the best of our knowledge, this natural material has not been used as a source of carbon materials for energy applications.

Many electrode types have been tested, and the most frequent systems today are synthesized on the electrochemical double-layer capacitor based on carbon and an organic electrolyte and convenient operability [22]. Yin et al. used KOH as an activator agent and coconut fibers to produce activated carbon to produce a supercapacitor electrode, which displayed a particular capacitance of 266 F/g at a current of 0.1 A/g. Many studies highlight the potential of crops and agricultural residues as a significant carbon source. Izan Izwan Misnon et al. used oil palm kernel shells to synthesize supercapacitors with outstanding performance. In comparison, those samples that were chemically activated represented a particular capacitance of 210 F/g at 0.5 A/g, while the same quality in physically activated samples was 50% lower [23].

2- Experimental

2-1- Synthesis

The raw material (leather leaf) was initially dried, and then the powder (3 g) was dissolved in water (50 mL) under stirring. The resulting solution was sealed into a Teflon-lined autoclave of 150 mL capacity, and maintained for 12 h and three different temperatures (100, 150, and 200 ºC) were applied in the hydrothermal carbonization stage, ensuring the complete progression of the reaction. After the autoclave was cooled to room temperature, the obtained hydrothermal carbon as dark precipitate was collected by centrifugation, washed with water and ethanol several times, and dried at 70 ºC for 8 h. The obtained hydrothermal carbon was mixed with the selected activation agents of KOH with the powder/ KOH weight ratio of 1:2. The mixture was heated up to 900 ºC temperature in a tube furnace under N_2 atmosphere for 2 h, with a temperature ramp of 5 ºC min^{-1}. The obtained activated carbon was washed with 2 M hydrochloric acid and water to remove potassium species thoroughly and finally dried at room temperature.

2-2- Characterization

The phase analysis of the samples was carried out via a Top metrology-GNR Explorer X-ray diffractometer (XRD, λ=0.154 nm, continuous scanning mode (0.02°/min)). Raman spectroscopy was also performed using a Raman Microscope (Teksan Co.) at room temperature in the wavelength range 45 to 4700 cm^{-1} on the Hamamatsu detection system and with the signal-to-noise ratio of 300:1 (estimated spectral resolution of 6 cm^{-1}). The sample excitement was aided by an Nd:YAG laser (785 nm with DPSS 785nm Laser, exposure time of 16s). The nitrogen adsorption-desorption method was applied in the mesostructural parameters investigations in which the samples were initially degassed at 353 K for 24 h. The Bruaauer–Emmett–Teller (BET) technique and Barrett–Joyner–Halenda (BJH) model were used in the measurements of specific surface area and pore diameters of the nano-carbon particles, respectively. The microstructural characterizations were carried out using a field-emission scanning electron microscope (FE-SEM, TESCAN Mira 3-XMU) and a transmission electron microscope (TEM, Philips CM120, operation voltage of 100 kV).

A ZIVE-SP1 potentiostat-galvanostat (Wonatech-Korea) was used in the electrochemical analysis of the samples. The test setup was designed as a three-electrode system, including a platinum wire as a counter electrode, saturated calomel as the reference electrode, and samples as the working electrodes. The working electrodes were prepared using a mixture of the synthesized carbon particles and silver paste, coated on cleaned FTO glass (1×1 cm^2) sheets. An aqueous solution of 0.5 M Na_2SO_4 was also applied as the electrolyte.

The cyclic voltammetry (CV) vs. SCE curves were then captured in the potential range of -0.2 to 0.5 V through the varying scan rates of 10 to 100 mV s^{-1}. The galvanostatic charge-discharge measurements were then carried out at 2-10 A g^{-1} over a voltage range of -0.2 to 0.5 V vs. SCE. The electrochemical impedance spectroscopy (EIS) measurements were also performed in the frequency range of 10^{-2} to 10^5 Hz at an open-circuit voltage (the amplitude of 0 V).

3- Results and discussion

The obtained hydrothermal carbon at three different temperatures (100, 150, and 200 ºC) are shown in Fig. 1. These powders were collected by centrifugation after the autoclave was cooled to room temperature. It can be observed that the best temperature is 200 ºC because the product color was not black in two other temperatures, indicating the carbon was not formed completely.

Fig. 1. Obtained hydrothermal carbon derived from the leather leaf at three different temperatures; a) 100, b) 150, and c) 200 ºC

The XRD pattern of nano-porous carbon spheres shown in Fig. 2 indicates two broad peaks around 23° and 43°. The peaks are respectively attributed to the (002) and (100) planes of the graphite-like carbon. However, based on the broadness of the peaks, the activated nano-porous carbon can be considered semi-crystalline materials.

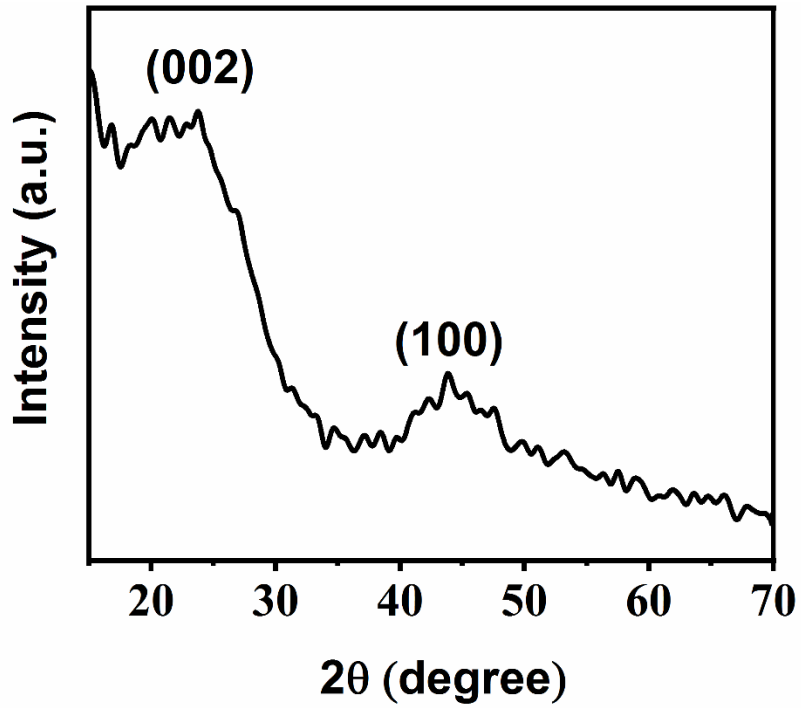

Fig. 2. X-ray diffraction (XRD) patterns of nanoporous carbon spheres derived from leather leaf

While the presence of graphitic structure in the obtained carbon particles cannot be well-indicated by the XRD, any ordered/disordered structure of the graphite flakes, known as a witness of graphene formation, can be detected via Raman spectroscopy. The typical Raman spectra of the activated nano-porous carbon particles are presented in Fig. 3. As can be seen, two peaks can be observed at 1320 and 1585 cm^{-1}, which are assigned to the characteristic D (defects and disorder) and G (graphitic) bands of carbon, respectively [24]. The G/D ratio of band intensities can be considered as an indicator of disordering and/or defects in the graphitic structure [25]. The G/D intensity ratio of carbon spheres was determined to be about 1.04. This result indicates that the porous carbons were relatively graphitized at low temperatures.

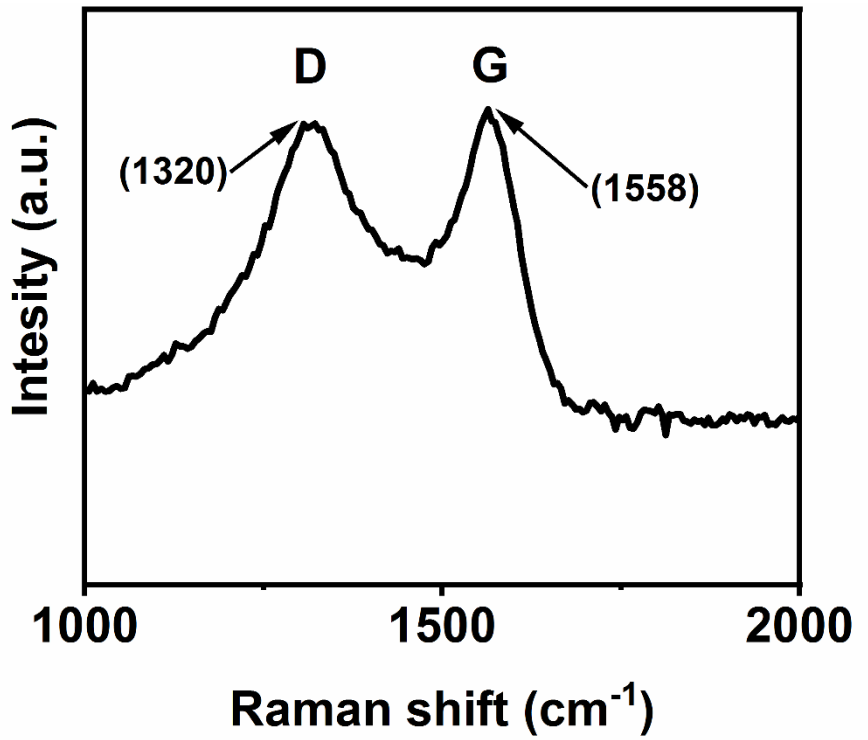

Fig. 3. Typical Raman spectra of the activated carbon particles obtained by hydrothermal carbonization

As shown in Fig. 4, the hydrothermal carbonization of leather leaf resulted in 2-5 µm diameter spherical carbon particles. This kind of spherical micro-sized particles was commonly observed for the hydrothermal carbons derived from mono- and polysaccharides (e.g., sucrose, glucose, starch, and cellulose) [26-29]. Upon KOH activation, the spherical morphology was still maintained in activated carbon, as evidenced by the SEM and the TEM images (Fig. 4 and 5). Fig. 5 shows the TEM image of the synthesized porous spheres with nanopores. These results reveal good stability of nanoporous carbon spheres, which are without any collapse during the high-temperature carbonization.

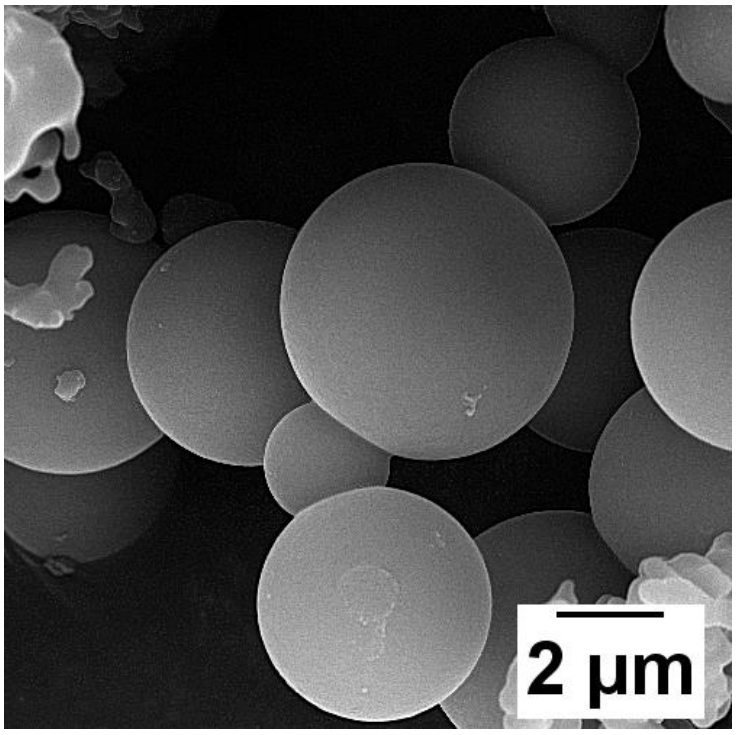

Fig. 4. FE-SEM images of nanoporous carbon spheres derived from leather leaf with spherical morphology

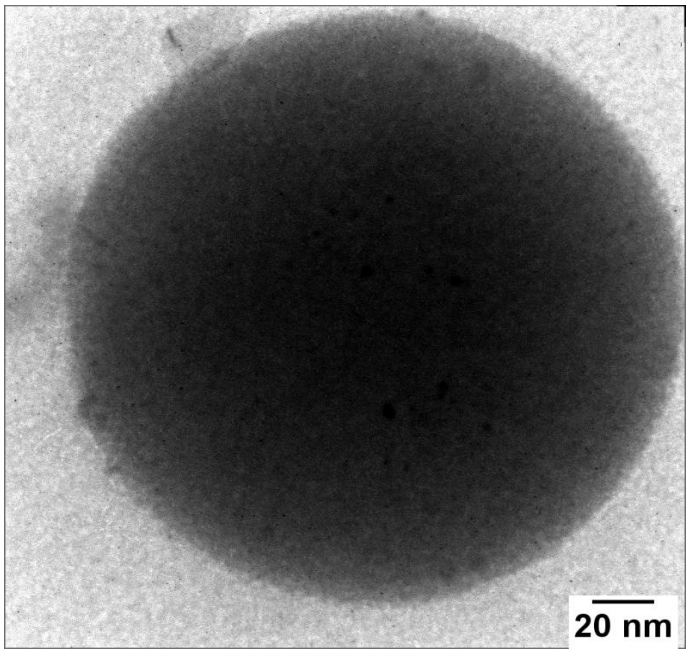

Fig. 5. TEM image of a single particle of nanoporous carbon

To further investigate the porosity, the surface area of the obtained nano-porous carbon particles was quantitatively measured through the Brunauer–Emmett–Teller (BET) method. Nitrogen adsorption-desorption isotherms of carbons are shown in Fig. 6. As can be seen, the adsorption isotherms are strongly dependent on the preparation conditions, which address the significance of the chemical activation process in controlling the surface area of the synthesized materials. The clear nitrogen uptakes, observed at low relative pressures ($P/P_0<0.1$), address the reversible type I isotherm that is commonly observed in microporous solids with relatively small external surfaces. Such limited uptake behavior is mainly derived by the volume of the accessible micro-pores rather than the internal surface area. Moreover, a slight increase in nitrogen uptake is observed at higher relative pressures. A small hysteresis loop was also observed at a higher relative pressure region. These situations have been often seen in nano-porous materials with randomly arranged pores having various sizes. The BET-specific surface area of nano-porous carbon spheres is calculated to be 1342 m^2g^{-1}.

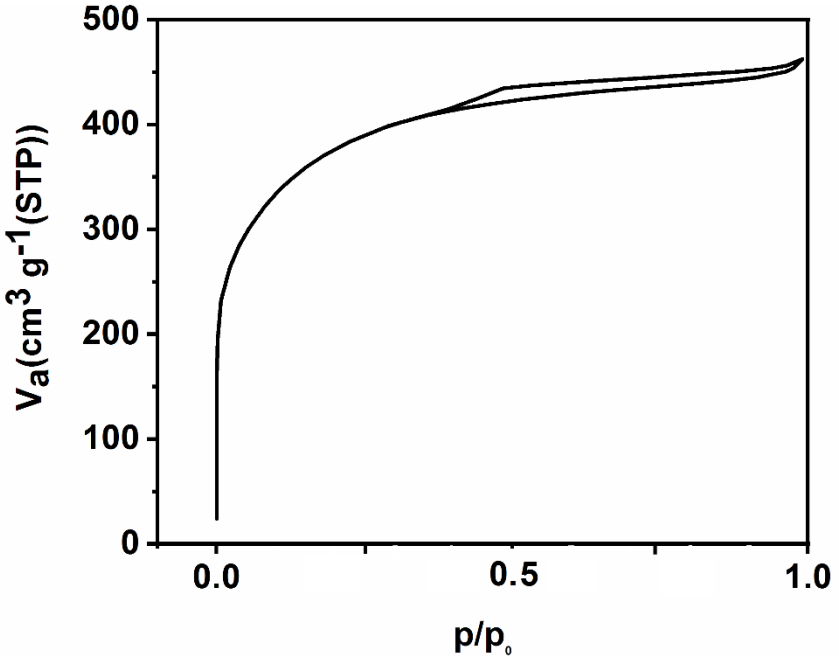

Fig. 6. Nitrogen adsorption and desorption isotherms measured at 77 K for the nanoporous carbon spheres

The pore size distribution (PSD) plot calculated by the Barrett-Joyner-Halenda (BJH) method is presented in Fig. 7. It resembles materials with narrow pore size distributions, a high ratio of micro-pores, and near mono-modal PSD curves with average diameters of 2 nm. Accordingly, smaller pores (1 ~ 2 nm) are detected in the carbon nano-spheres obtained from the KOH-activated samples.

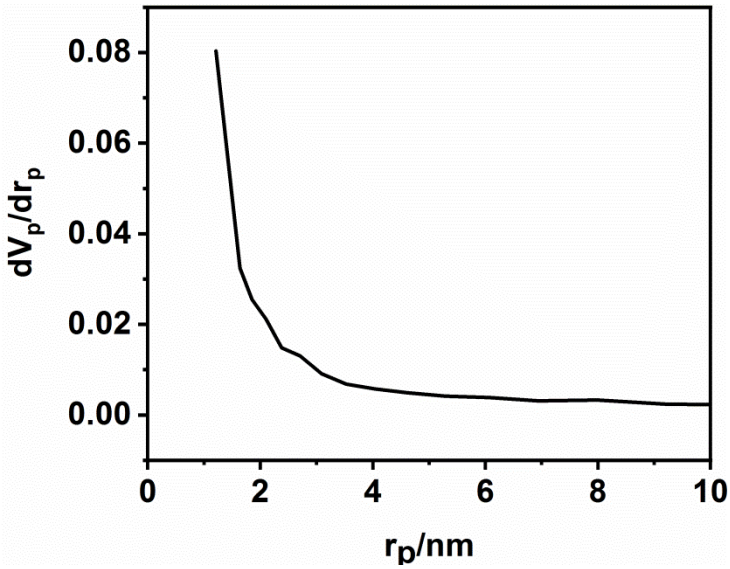

Fig. 7. Barrett-Joyner-Halenda (BJH) pore size distributions isotherm of nanoporus carbon spheres

The electrochemical capacitive properties of leather leaf-derived carbon materials were measured in 0.5 M Na_2SO_4 electrolyte using a three-electrode system. Fig. 8 depicts the CV curves of the carbon at the scan rate ranging from 10 to 100 mV s^{-1}. The relatively rectangular-shaped CV curves of all the activated carbons resemble the typical characteristic of double-layer capacitance. Moreover, as shown in Fig. 8, the porous carbon still presents a relatively rectangular CV shape at a high scan rate of 100 mV s^{-1}, which confirms the efficient charge transfer and electrolyte diffusion within the nanoporous carbon spheres [30].

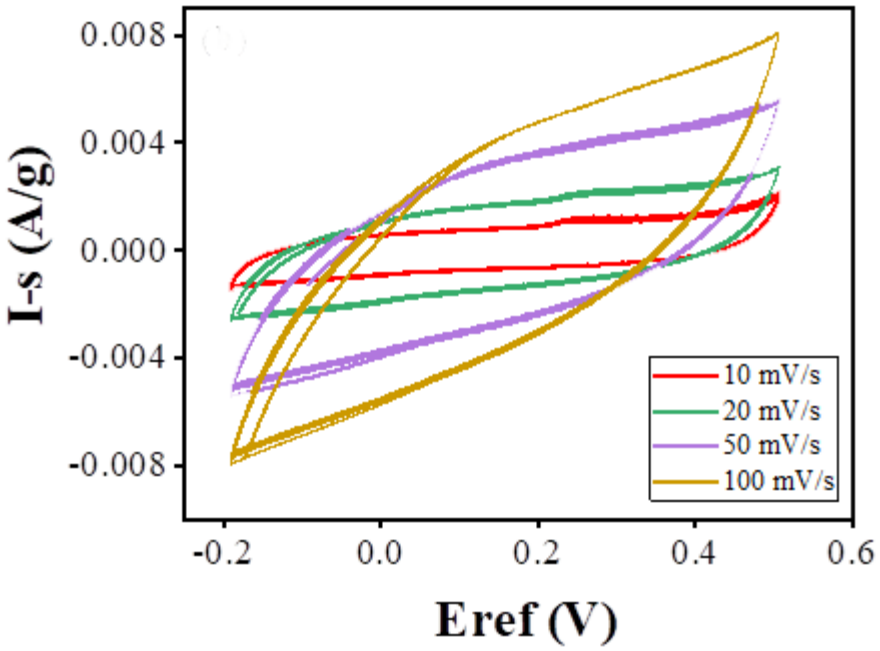

Fig. 8. Cyclic voltammetry (CV) curves of carbon spheres at various scan rate ranging from 10 to 100 mV s^{-1}

The galvanostatic charge-discharge curves of the carbons at a current density of 2 A g^{-1} are shown in Fig. 9. The relatively triangular shape curves indicate good reversibility of the carbon materials. The specific capacitance was calculated according to the following equation: $C=i\Delta t/m\Delta V$, where i is discharge current (A), Δt is discharge time (s), and ΔV is a potential window (V) [31, 32]. The obtained specific capacitances value is 374 F g^{-1}.

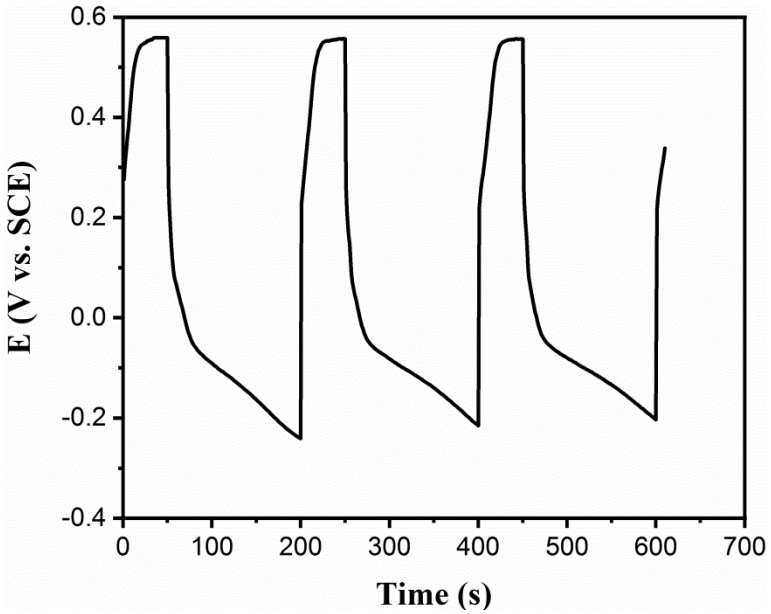

Fig. 9. Galvanostatic charge-discharge curves (chronopotentiometry) of the nanoporous carbons

Fig. 10 shows the Nyquist plots of carbons in the frequency range of 10^{-2} to 10^{5} Hz under open circuit potential. As can be seen, the nanoporous carbon particles show good capacitive behavior, including a vertical slope at the low-frequency region. At higher frequencies, the intercept of the plot with the real axis represents the equivalent series resistance (ESR) Rs, which is occurred due to the combination of the effects of ionic resistance of the electrolyte, intrinsic resistance of the active materials, and contact resistance with the current collector [33]. At medium frequencies, Nyquist plots exhibit a Warburg-type line with a slope of about 45°. Projecting the length of the Warburg line on the real axis can result in increased diffusion of ions at the electrode-electrolyte interface [34]. As shown in Fig. 9, the carbon spheres demonstrate the short Warburg-type line, indicating superior ion diffusion in the mesoporous structure of carbon spheres.

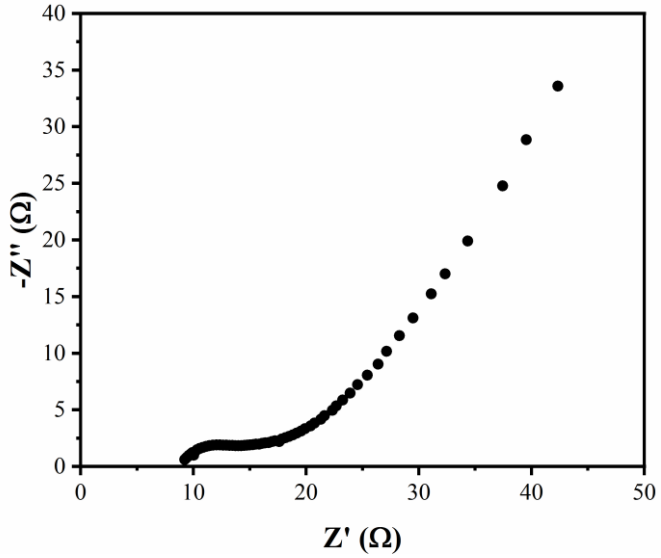

Fig. 10. Electrochemical impedance spectra (EIS) or Niquist plot of the activated carbons

4. Conclusion

Nano-porous carbon spheres have been successfully synthesized via a template-free hydrothermal assisting pyrolysis method using the leather leaf as a low-cost precursor material. Results showed that the best temperature for the hydrothermal stage is 200 ºC. Compared with the products obtained by single hydrothermal treatment or annealing treatment, the carbon spheres have the largest specific surface area, exhibit suitable electric double-layer capacitance. The results of porosimetry through the N_2 adsorption-desorption method indicated the highest surface area of 1342 m^2g^{-1}.

The rectangular shape of the CV curves in this study showed the typical characteristics of double-layer capacitance. Notably, the synthesized carbon particles derived by the KOH activation agents presented a high capacitance of 374 F g^{-1}. The superior capacitive properties of carbon spheres are closely related to their high surface area, optimized microporous structure, and narrow pore size distribution. This work demonstrates that the textural properties of carbon materials derived from biomass can be finely modulated by KOH activation. The leather-leaf derived carbon sphere materials have promising potential in the application of energy storage devices.

References

[1] Y. Yang, M. Luo, W. Zhang, Y. Sun, X. Chen, S. Guo, "Metal surface and interface energy electrocatalysis: Fundamentals, performance engineering, and opportunities", Chem, Vol. 4, No. 9, 2018, pp. 2054-2083.

[2] S. Zhang, Q. Fan, R. Xia, T.J. Meyer, "Co2 reduction: From homogeneous to heterogeneous electrocatalysis", Accounts of Chemical Research, Vol. 53, No. 1, 2020, pp. 255-264.

[3] C. Touriño, F. Oveisi, J. Lockney, D. Piomelli, R. Maldonado, "Faah deficiency promotes energy storage and enhances the motivation for food", Int J Obes (Lond), Vol. 34, No. 3, 2010, pp. 557-68.

[4] Y.S. Yun, M.H. Park, S.J. Hong, M.E. Lee, Y.W. Park, H.J. Jin, "Hierarchically porous carbon nanosheets from waste coffee grounds for supercapacitors", ACS Appl Mater Interfaces, Vol. 7, No. 6, 2015, pp. 3684-90.

[5] R. Srinivasan, E. Elaiyappillai, H.P. Pandian, R. Vengudusamy, P.M. Johnson, S.-M. Chen, R. Karvembu, "Sustainable porous activated carbon from polyalthia longifolia seeds as electrode material for supercapacitor application", Journal of Electroanalytical Chemistry, Vol. 849, No. 2019, pp. 113382.

[6] J.P. Paraknowitsch, Y. Zhang, B. Wienert, A. Thomas, "Nitrogen- and phosphorus-co-doped carbons with tunable enhanced surface areas promoted by the doping additives", Chemical Communications, Vol. 49, No. 12, 2013, pp. 1208-1210.

[7] H. Zhang, J. Chen, Y. Li, P. Liu, Y. Wang, T. An, H. Zhao, "Nitrogen-doped carbon nanodots@nanospheres as an efficient electrocatalyst for oxygen reduction reaction", Electrochimica Acta, Vol. 165, No. 2015, pp. 7-13.

[8] S. Chao, Q. Cui, K. Wang, Z. Bai, L. Yang, J. Qiao, "Template-free synthesis of hierarchical yolk-shell co and n codoped porous carbon microspheres with enhanced performance for oxygen reduction reaction", Journal of Power Sources, Vol. 288, No. 2015, pp. 128-135.

[9] M. Li, H. Xiao, T. Zhang, Q. Li, Y. Zhao, "Activated carbon fiber derived from sisal with large specific surface area for high-performance supercapacitors", ACS Sustainable Chemistry & Engineering, Vol. 7, No. 5, 2019, pp. 4716-4723.

[10] R. Wang, P. Wang, X. Yan, J. Lang, C. Peng, Q. Xue, "Promising porous carbon derived from celtuce leaves with outstanding supercapacitance and co_2 capture performance", ACS Appl Mater Interfaces, Vol. 4, No. 11, 2012, pp. 5800-6.

[11] S. Yaglikci, Y. Gokce, E. Yagmur, Z. Aktas, "The performance of sulphur doped activated carbon supercapacitors prepared from waste tea", Environmental Technology, Vol. 41, No. 1, 2020, pp. 36-48.

[12] B. Zhu, C. Shang, Z. Guo, "Naturally nitrogen and calcium-doped nanoporous carbon from pine cone with superior co2 capture capacities", ACS Sustainable Chemistry & Engineering, Vol. 4, No. 3, 2016, pp. 1050-1057.

[13] J. Tang, J. Liu, N.L. Torad, T. Kimura, Y. Yamauchi, "Tailored design of functional nanoporous carbon materials toward fuel cell applications", Nano Today, Vol. 9, No. 3, 2014, pp. 305-323.

[14] P. Liu, Y. Wang, J. Liu, "Biomass-derived porous carbon materials for advanced lithium sulfur batteries", Journal of Energy Chemistry, Vol. 34, No. 2019, pp. 171-185.

[15] S. Gao, Y. Chen, H. Fan, X. Wei, C. Hu, H. Luo, L. Qu, "Large scale production of biomass-derived n-doped porous carbon spheres for oxygen reduction and supercapacitors", Journal of Materials Chemistry A, Vol. 2, No. 10, 2014, pp. 3317-3324.

[16] R. Liu, D. Wu, X. Feng, K. Müllen, "Nitrogen-doped ordered mesoporous graphitic arrays with high electrocatalytic activity for oxygen reduction", Angew Chem Int Ed Engl, Vol. 49, No. 14, 2010, pp.

2565-9.
[17] P.A. Lovell, F.J. Schork, "Fundamentals of emulsion polymerization", Biomacromolecules, Vol. 21, No. 11, 2020, pp. 4396-4441.
[18] D. Kim, K. Lee, K. Park, "Upgrading the characteristics of biochar from cellulose, lignin, and xylan for solid biofuel production from biomass by hydrothermal carbonization", Journal of Industrial and Engineering Chemistry, Vol. 42, No. 2016, pp. 95-100.
[19] A.Y. Krylova, V.M. Zaitchenko, "Hydrothermal carbonization of biomass: A review", Solid Fuel Chemistry, Vol. 52, No. 2, 2018, pp. 91-103.
[20] X. Xu, E. Jiang, "Treatment of urban sludge by hydrothermal carbonization", Bioresour Technol, Vol. 238, No. 2017, pp. 182-187.
[21] S. Nizamuddin, H.A. Baloch, G.J. Griffin, N.M. Mubarak, A.W. Bhutto, R. Abro, S.A. Mazari, B.S. Ali, "An overview of effect of process parameters on hydrothermal carbonization of biomass", Renewable and Sustainable Energy Reviews, Vol. 73, No. 2017, pp. 1289-1299.
[22] K. Mensah-Darkwa, C. Zequine, P.K. Kahol, R.K. Gupta, "Supercapacitor energy storage device using biowastes: A sustainable approach to green energy", Sustainability, Vol. 11, No. 2, 2019, pp. 414.
[23] L. Yin, Y. Chen, D. Li, X. Zhao, B. Hou, B. Cao, "3-dimensional hierarchical porous activated carbon derived from coconut fibers with high-rate performance for symmetric supercapacitors", Materials & Design, Vol. 111, No. 2016, pp. 44-50.
[24] I.I. Misnon, N.K.M. Zain, R.A. Aziz, B. Vidyadharan, R. Jose, "Electrochemical properties of carbon from oil palm kernel shell for high performance supercapacitors", Electrochimica Acta, Vol. 174, No. 2015, pp. 78-86.
[25] Y. Fan, X. Yang, B. Zhu, P.-F. Liu, H.-T. Lu, "Micro-mesoporous carbon spheres derived from carrageenan as electrode material for supercapacitors", Journal of Power Sources, Vol. 268, No. 2014, pp. 584-590.
[26] A.C. Ferrari, J. Robertson, "Interpretation of raman spectra of disordered and amorphous carbon", Physical Review B, Vol. 61, No. 20, 2000, pp. 14095-14107.
[27] C.A. Nieves, L.M. Martinez, A. Meléndez, M. Ortiz, I. Ramos, N.J. Pinto, N. Zimbovskaya, "Temperature-dependent charge transport mechanisms in carbon sphere/polyaniline composite", AIP Advances, Vol. 7, No. 12, 2017, pp. 125229.
[28] G. Wen, B. Wang, C. Wang, J. Wang, Z. Tian, R. Schlögl, D.S. Su, "Hydrothermal carbon enriched with oxygenated groups from biomass glucose as an efficient carbocatalyst", Angewandte Chemie International Edition, Vol. 56, No. 2, 2017, pp. 600-604.
[29] J. Serrano, P. Pico, M. Amín, A. Pinilla, D. Torrado, C. Murillo, N. Bardin-Monnier, N. Ratkovich, F. Muñoz, O. Dufaud, "Experimental and cfd-dem study of the dispersion and combustion of wheat starch and carbon-black particles during the standard 20l sphere test", Journal of Loss Prevention in the Process Industries, Vol. 63, No. 2020, pp. 103995.
[30] S. Yu, W. Li, Y. Fujii, T. Omura, H. Minami, "Fluorescent spherical sponge cellulose sensors for highly selective and semiquantitative visual analysis: Detection of hg2+ and cu2+ ions", ACS Sustainable Chemistry & Engineering, Vol. 7, No. 23, 2019, pp. 19157-19166.
[31] H. Yang, "Graphene-based supercapacitors for energy storage applications", Proc. 2013, pp.
[32] X. Liu, M. Zheng, Y. Xiao, Y. Yang, L. Yang, Y. Liu, B. Lei, H. Dong, H. Zhang, H. Fu, "Microtube bundle carbon derived from paulownia sawdust for hybrid supercapacitor electrodes", ACS Applied Materials & Interfaces, Vol. 5, No. 11, 2013, pp. 4667-4677.
[33] I. Gaztelumendi, M. Chapartegui, R. Seddon, S. Flórez, F. Pons, J. Cinquin, "Enhancement of electrical conductivity of composite structures by integration of carbon nanotubes via bulk resin and/or buckypaper films", Composites Part B: Engineering, Vol. 122, No. 2017, pp. 31-40.
[34] L. Sun, C. Tian, M. Li, X. Meng, L. Wang, R. Wang, J. Yin, H. Fu, "From coconut shell to porous graphene-like nanosheets for high-power supercapacitors", Journal of Materials Chemistry A, Vol. 1, No. 21, 2013, pp. 6462-6470.